Korean J. Chem. Eng., 40(8), 1919-1927 (2023)
DOI: 10.1007/s11814-023-1407-1

pISSN: 0256-1115
eISSN: 1975-7220

Sludge deep dewatering enhanced by zero-valent iron/peroxymonosulfate/walnut shell powder

Yanping Zhang*,†, Miaolin He*, Xieping Xue*, Fen Li, Ning Lv*, and Jinghao Dong****

*School of Civil Engineering and Transportation, Hebei University of Technology, Tianjin 300401, China
**School of Materials Science and Chemical Engineering, Harbin University of Science and Technology, Harbin 150040 , Heilongjiang, China

(*Received 25 August 2022 • Revised 30 January 2023 • Accepted 27 February 2023*)

Abstract−To enhance sludge dewatering performance, Zero-valent iron/peroxymonosulfate/walnut shell powder was used to condition sludge at 55 °C and pH=3 (ZVI/PMS/WSP-T/pH), and the dewatering mechanism was also analyzed. The results showed that the capillary suction time (CST) and water content of sludge cake (W_c) were reduced to 6.8 s and 62.1%, respectively, and net sludge yield (Y_N) increased to 58.74 kg/(m^2·h) after being treated by ZVI/PMS/WSP-T/pH. The thermal and acid conditions could promote the corrosion of Fe^{2+} from ZVI and enhance PMS to produce more $SO_4^{-\bullet}$ and ·OH. The radicals combined with acid and thermal hydrolysis could efficiently reduce extracellular polymeric substances (EPS), especially tightly bound EPS (TB-EPS), destroy sludge floc and release bound water. The stripping off of EPS and neutralization of Fe^{3+}, Fe^{2+} and H^+ caused the zeta potential to increase to −0.91 mV. The flocculation of cations and adsorption of WSP further increased the fractal dimension to 1.71. Moreover, the rigid and porosity structure of WSP increased sludge incompressibility and formed channels for water. Under the combined oxidation, acid/thermal hydrolysis, re-aggregation and skeleton builder functions, the sludge dewatering performance was greatly improved.

Keywords: Sludge Dewatering, Zero Valent Iron, Peroxymonosulfate, Walnut Shell, Extracellular Polymeric Substances

INTRODUCTION

With the development of industry and urbanization, more and more wastewater treatment plants have been built to protect the aquatic environment. Waste activated sludge (WAS) as a byproduct of biological treatment in wastewater treatment plants is also increasing. It is estimated that the annual sludge production will be up to 90 million tons (80% water content) until 2025 [1]. WAS needs to be treated adequately because it can contain harmful materials, such as heavy metals, refractory organic compounds and pathogenic microorganisms [2,3]. However, due to the high water content, WAS has a large volume, which increases the cost of transportation and treatment [4]. Moreover, many sludge disposal technologies, such as incineration, landfill and utilization for building materials, require the water content of sludge to be reduced to a certain extent [2]. Therefore, deep sludge dewatering is essential for sludge final disposal. It was reported that the main water types in sludge are free water, interstitial water, and bound water [5]. Free water can be separated easily from sludge by gravity or mechanically, while bound water removal is more difficult and thus requires energy to convert it into free water [6]. Meanwhile, the sludge cells are coated with a layer of extracellular polymeric substances (EPS), with strong hydrophilicity and a biogel structure, containing large amounts of bound water. It was reported that the distribution of different EPS components has an essential impact on the sludge dewaterability [7]. Therefore, oxidation technologies using sodium periodate [8], Fenton [9], persulfate [10], ozone oxidation [11] and photocatalytic oxidation [12] have been employed recently to destroy EPS structures to improve sludge dewaterability.

Sulfate radical $SO_4^{-\bullet}$ oxidation technology has been focused on sludge treatment in recent years due to its high redox potential, low cost and harmless end-product (SO_4^{2-}) [13]. It was reported that $SO_4^{-\bullet}$ can efficiently destroy the structure of EPS and sludge floc, and release bound water, and then enhance sludge dewaterability [14]. Peroxydi- and monosulfate (PDS and PMS) are two main precursors of $SO_4^{-\bullet}$. Compared to PDS, PMS has asymmetric structure and can more easily produce $SO_4^{-\bullet}$ [15]. Zero-valent iron (ZVI) is usually used to active PMS to produce $SO_4^{-\bullet}$ due to being environmentally friendly and low cost [14]. However, under neutral conditions and room temperature, the activation rate of ZVI for PMS can be slow due to the low dissolution rate of Fe^{2+} from ZVI. On the other hand, an oxide iron layer rapidly forms at the ZVI surface during the reaction, which could further limit the release of Fe^{2+} from ZVI [16]. This could weaken the oxidation capacity of the system, resulting in low sludge dewatering performance. To overcome these drawbacks, reducing agents and chelating agents, such as ascorbic acid [17] and nitrilotriacetic acid [18], were introduced to ZVI-based advanced oxidation process to improve activation performance. However, these chemical agents are usually toxic and cause secondary pollution. Therefore, how to enhance the activation efficiency of ZVI for persulfate and improve sludge dewaterability should be focused.

†To whom correspondence should be addressed.
E-mail: zyphit@hebut.edu.cn

On the other hand, sludge is highly compressible and deforms under high-pressure filtration [19]. Mainly when excessive oxidation occurs, a large amount of EPS dissolves out, the viscosity and compressibility of sludge increases and the sludge dewaterability deteriorates [20]. Therefore, skeleton builders, such as gypsum [21], powdered lime [22], rice husk [15] and biochar [23], have been used to construct water filtering channels during pressure filtration to enhance sludge dewatering. Walnut shell is an abundant biomass material, and its production reaches 2,000,000 tons per year [24]. It has high hardness and can be used as a filter aid to form a permeable, porous and rigid frame structure during sludge dewatering, and the biomass material itself is conducive to the reuse of sludge.

It is known that thermal and acid both can activate PMS to produce radicals [25]. However, it is not clear whether they can promote the dissolution of Fe^{2+} from ZVI and improve the oxidation efficiency of ZVI/PMS system. Therefore, they were combined with ZVI to enhance the corrosion of Fe^{2+} to activate PMS, and then WSP was added as a skeleton builder to improve sludge dewaterability in this study. This method does not introduce additional toxic chemicals and is beneficial to the subsequent resource utilization of dewatered sludge. After being conditioned by ZVI/PMS/WSP-T/pH, the capillary suction time (CST), the water content of sludge cake (W_c) and net sludge yield (Y_N) were measured to evaluate sludge dewaterability. Moreover, scanning electron microscopy (SEM), zeta potential, extracellular polymeric substances (EPS) and sludge fractal dimension were further used to reveal the dewatering mechanism, and the results were compared with raw sludge and those by WSP, ZVI/PMS, ZVI/PMS-T and ZVI/PMS -T/pH.

MATERIALS AND METHODS

1. Materials

The sludge sample was supplied by a wastewater treatment plant in Tianjin, China. The obtained sludge was concentrated to ~11,000 mg/L and stored at 4 °C before experiments. The experiment was completed within three days. The properties of raw sludge were as follows: pH 6.74±0.1, total solid (TS) 11,000±1,000 mg/L, CST 19.8±1.3 sec, SRF 12.4±0.1×10^{12} m/kg, W_c 98.4±0.2% and ORP −8.53±0.2 mV. The walnut shell was crushed, ground and sieved and then stored at ambient temperature for further use after oven-drying at 105 °C for 2 h. The particle size grading of WSP was: 15%<0.075 mm, 20% 0.075-0.15 mm, 50% 0.15-0.3 mm and 15%>0.3 mm. ZVI, $KHSO_5$ and other chemical reagents used in the experiment were all analytically pure.

2. Experimental Methods

First, a 300 mL sludge sample was placed into a 500-mL glass beaker. The pH of the raw sludge sample was adjusted to pH 3 using 0.1 mol/L HCl, and then the beaker was placed into a water bath with 55 °C. After the sample's temperature was stable, 210 mg/g TS ZVI and 70 mg/g TS PMS were added to the sludge sample (the dosages of ZVI and PMS were determined from our previous single factor experiment), and then the sludge solution was continuously stirred for 60 min at 150 rpm. After that, 400 mg/g TS WSP with specific particle size gradation (15% <0.075 mm, 20% 0.075-0.15 mm, 50% 0.15-0.3 mm, 15% >0.3 mm) was added into the beaker. The mixture was continuously stirred at 150 rpm for 10 min. This conditioning process resulted in the sample being marked as ZVI/PMS/WSP-T/pH.

After conditioning by ZVI/PMS/WSP-T/pH, the unused ZVI was retrieved by magnetic force, and then CST, W_c, Y_N, SEM, compression coefficient, zeta potential, EPS and sludge fractal dimension were measured. The sludge treated by WSP, ZVI/PMS, ZVI/PMS-T, and ZVI/PMS-T/pH was also performed, and the corresponding experimental conditions are detailed in Table 1.

3. Analytical Methods

The CST was measured by a DFC-10A CST instrument (China). W_c was determined according to the Standard Methods [26] after undergoing vacuum filtration (0.1 MPa for 5 min); TSS, Fe^{3+} and Fe^{2+} were determined according to the Standard Methods [26]. The pH was determined by a digital pH meter (pHSJ-4A, China). Zeta potential was measured by a Zetasizer Nano ZS Instrument (England). The morphology of the sludge cake treated by different methods was investigated via scanning electron microscopy (Nova Nano SEM 450, America). The EPS of sludge was investigated by the thermal treatment method [27]. Soluble protein was determined by the Coomassie brilliant blue G250 method with Bull Serum Albumin (BSA) as the standard [28], while soluble polysaccharide was determined by the phenol-sulfuric method with glucose as the standard [29,30].

The fractal dimension was determined as follows: sludge sample was placed on the glass slide, observed and photographed after magnification with an XSP-8CC biological microscope (China). The obtained photos of flocs were processed with Image-Pro software to calculate its area (A) and perimeter (P). According to Eq. (1) [31], the two-dimensional fractal dimension of sludge flocs can be calculated. For each D_f calculation, at least 24 flocs from the image were analyzed.

Table 1. The experimental protocol of different treatment conditions

Order	Conditions	T (°C)	pH	Dosage (mg/gTS)		
				ZVI	PMS	WSP
1	RAW	25	6.74	0	0	0
2	WSP	25	6.74	0	0	400
3	ZVI/PMS	25	6.74	210	70	0
4	ZVI/PMS-T	55	6.74	210	70	0
5	ZVI/PMS-T/pH	55	3.00	210	70	0
6	ZVI/PMS/WSP-T/pH	55	3.00	210	70	400

$$A \propto P^{D_f} \quad (1)$$

The coefficient of compressibility (s) can be calculated using an empirical formula, as Eq. (2) [32]:

$$\frac{SRF_i}{SRF_0} = \left[\frac{P_i}{P_0}\right]^s \quad (2)$$

where P_i is the actual pressure (Pa); P_0 is the reference pressure (Pa); SRF_i is the specific resistance to filtration (SRF) corresponding to actual pressure (s^2/g); SRF_0 is the SRF corresponding to reference pressure (s^2/g). SRF was measured by a TG-250 specific resistance tester (China).

Net sludge yield (Y_N) was calculated according to Eq. (3) and Eq. (4) [23]:

$$Y_N = F\left(\frac{2p\omega}{\mu t}\cdot\frac{1}{SRF}\right)^{\frac{1}{2}} \quad (3)$$

$$F = \frac{SS_{original}}{SS_{original}+SS_{conditioned}} \quad (4)$$

where Y_N is the Net sludge yield ($kg/(m^2 \cdot h)$); F is the correction factor; t is the filtration time (s), p is filtration pressure (Pa), ω is dry solid mass retained on filter medium by per unit volume filtrate, μ is dynamic viscosity coefficient of filtrate ($kg \cdot s/m^3$), $SS_{original}$ is the mass of the solid per liter of raw sludge, $SS_{conditioned}$ is the mass of the solid per liter of conditioned sludge.

RESULTS AND DISCUSSION

1. Effect of ZVI/PMS/WSP-T/pH on Sludge Dewatering Performance

The effect of ZVI/PMS/WSP-T/pH on sludge dewatering performance was studied, and the results were compared with those treated by WSP, ZVI/PMS, ZVI/PMS-T and ZVI/PMS-T/pH (Fig. 1). As illustrated in Fig. 1(a), raw sludge presented inferior dewatering performance with a CST of 19.8 s and W_c of 85.1%. The sludge dewaterability increased when treated by WSP, ZVI/PMS, ZVI/PMS-T, ZVI/PMS-T/pH and ZVI/PMS/WSP-T/pH. The sludge dewatering performance was the highest when conditioned with ZVI/PMS/WSP-T/pH. Compared to sludge treated by ZVI/PMS process, the CST and W_c decreased from 14.7 s and 80.5% to 6.8 s and 62.1%, respectively. This result was also better than that by ZVI/PS treatment reported in literature. For example, Li et al. [33] reported that under the treatment 0.5 g/g TSS persulfate and 2 g/g TSS ZVI, the CST and W_c of the anaerobically digested sludge were 8.6 s and 71.2%, respectively. While Zhou et al. [34] achieved 50% CST reduction, as CST was 10.3 s, when the addition of persulfate and ZVI was 4 g/L and 15 g/L, respectively. The highest sludge dewatering performance was obtained due to the following reasons:

(1) ZVI could activate PMS to produce $SO_4^{-\bullet}$ with strong oxidation and reductive Fe^{2+} (Eq. (5)), and the Fe^{2+} also could activate PMS to produce more $SO_4^{-\bullet}$ through Eq. (6). In addition, ZVI also could activate PMS to produce hydroxyl radical (·OH) and Fe^{3+} through Eq. (7) [35]. The reactive species ($SO_4^{-\bullet}$ and ·OH) could destroy the structure of sludge floc and EPS, which wrapped around the sludge cell, and Fe^{3+} could re-flocculate the broken sludge floc. The combined oxidation and re-flocculation function caused the bound water to be released, and sludge dewatering performance improved;

(2) High temperature (T=55 °C) can accelerate the yields of $SO_4^{-\bullet}$ and ·OH through Eq. (8), and thermal and low pH values (pH=3) were conducive to the dissolution of Fe^{2+} from ZVI (Eq. (9)), and then accelerate the formation of $SO_4^{-\bullet}$ (Eq. (6)) to destroy the EPS structure [36]. Furthermore, the acidic and thermal conditions could disintegrate EPS, causing the interstitial water and bound water convert into free water, hence improving sludge dewatering performance [4,37]. Therefore, the sludge dewatering performance obtained by ZVI/PMS-T/pH was higher than that by ZVI/PMS, and the CST and W_c decreased to 7.8 s, and 70.4%, respectively;

(3) WSP could act as a skeleton builder to form pore structure and provide channels for free water during filtration pressure, which further improved the sludge dewatering performance.

$$Fe^0 + HSO_5^- + H^+ \rightarrow Fe^{2+} + SO_4^{-\bullet} + H_2O \quad (5)$$

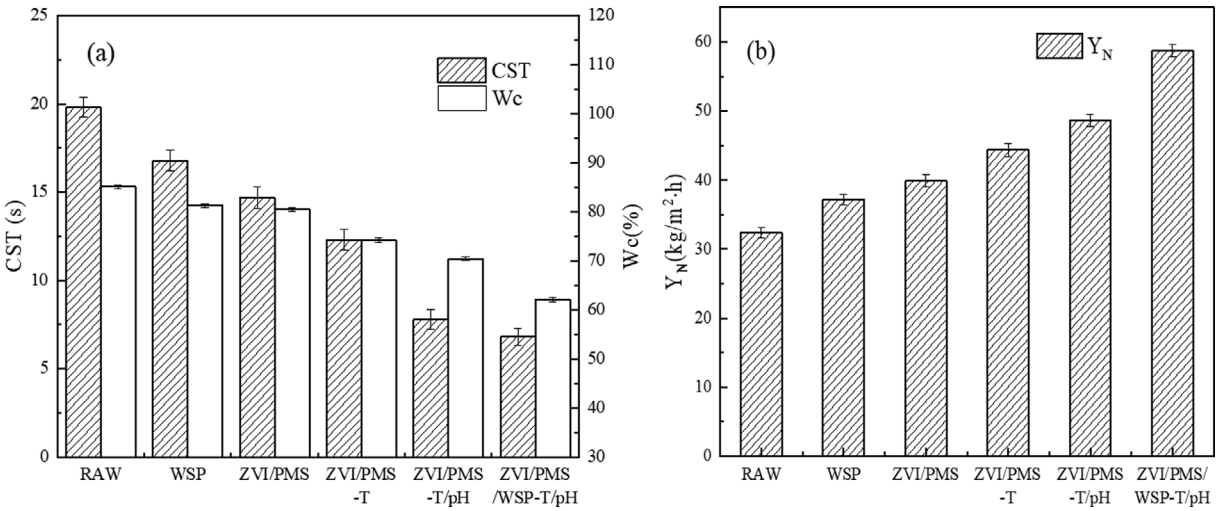

Fig. 1. The dewatering performance (a) and the net sludge yield (b) of sludge conditioned by different treatment methods.

$$Fe^{2+}+HSO_5^-\rightarrow Fe^{3+}+SO_4^{-\bullet}+OH^- \quad (6)$$

$$Fe^0+HSO_5^-\rightarrow Fe^{3+}+SO_4^{2-}+\cdot OH \quad (7)$$

$$HSO_5^-+Heat\rightarrow SO_4^{-\bullet}+\cdot OH \quad (8)$$

$$2Fe^0+O_2+2H_2O\rightarrow 2Fe^{2+}+4OH^- \quad (9)$$

Considering that the solid content of sludge would increase after adding WSP as a skeleton builder, the index of net sludge yield (Y_N) was further investigated to evaluate the sludge filtration and dewatering performance [36]. The Y_N represents the quantity of sludge solids filtered per unit time and filtration area. The higher the Y_N value, the better filtration performance and sludge dewaterability. The values of Y_N at different treatment methods were measured, and the results are shown in Fig. 1(b). It was shown that the Y_N of raw sludge was 32.40 kg/(m^2·h), and its value increased in turn to 37.16, 39.85, 44.37, 48.66 and 58.74 kg/(m^2·h) when treated by WSP, ZVI/PMS, ZVI/PMS-T, ZVI/PMS-T/pH and ZVI/PMS/WSP-T/pH. It showed an opposite trend when compared with that of Wc and CST. This result indicated that the sludge filtration performance and sludge dewaterability were enhanced after being treated by ZVI/PMS/WSP-T/pH.

2. Morphological Structure of Sludge Cake

The morphological structure of sludge cake treated by ZVI/PMS/WSP-T/pH was characterized by SEM and the result was compared with those by WSP, ZVI/PMS, ZVI/PMS-T and ZVI/PMS-T/pH (Fig. 2). It can be observed from Fig. 2(a) that the raw sludge had a glutinous structure induced by EPS with a relatively smooth and compact surface, resulting in poor dewaterability of sludge. The sludge floc kept its initial gel structure when treated by WSP (Fig. 2(b)) due to WSP only could play as a skeleton builder, and the bound water could not be released. While the sludge cake became rough, a few clearances appeared when treated by ZVI/PMS (Fig. 2(c)). It was because that $SO_4^{-\bullet}$ and ·OH were produced under this condition, and the EPS was denudated, or the strong oxidation of $SO_4^{-\bullet}$ and/or ·OH destroyed some sludge cells. When increasing the temperature to 55 °C (ZVI/PMS-T), the surface of the sludge cake after conditioning became rough and with higher porosity, and the gel structure composed of EPS was destroyed, even the sludge cell was broken (Fig. 2(d)). This was conducive to the release of bound water. Moreover, the cracks and holes could provide channels for water, improving the permeability of sludge cake [38]. The strong disintegration effect was likely owing to the iron corrosion rate being accelerated at higher temperatures, and more free radicals were produced under the combined activation of Fe^{2+} and thermal for PMS [39], and also the thermal hydrolysis of sludge. Smaller cracks and holes disappeared when the pH was adjusted to 3 (ZVI/PMS-T/pH). At the same time, some irregular granular objects appeared, which formed amorphous minerals crystals during the reaction. However, we know that the sludge dewaterability was good under this condition (Fig. 1(a)). It might be that under acidic conditions, more flocculants, such as Fe^{3+} or Fe^{2+}, were generated, which could re-flocculate the broken sludge floc to form larger "aggregates" and destabilize the sludge. When WSP (ZVI/PMS/WSP-T/pH) was added, the raised irregular particles were hidden in the sludge cake structure, and the sludge floc became larger. It may be that WSP had a specific adsorption and aggregation effect on sludge flocs [40], and the addition of WSP could wrap some minerals. However, the sludge surface differed from raw sludge, and the gel structure caused by EPS disappeared. The results above show that the sludge experienced a comprehensive pre-oxidation process to release bound water, re-flocculation and skeleton construction when treated by ZVI/PMS/WSP-T/pH, which significantly improved sludge dewaterability.

3. Sludge Compressibility

The compression coefficient, s, of sludge cake could reflect the compression performance of sludge [41]. Sludge usually has a high value of s and is prone to compression deformation because it contains numerous hydrophilic particles [42]. This will block the

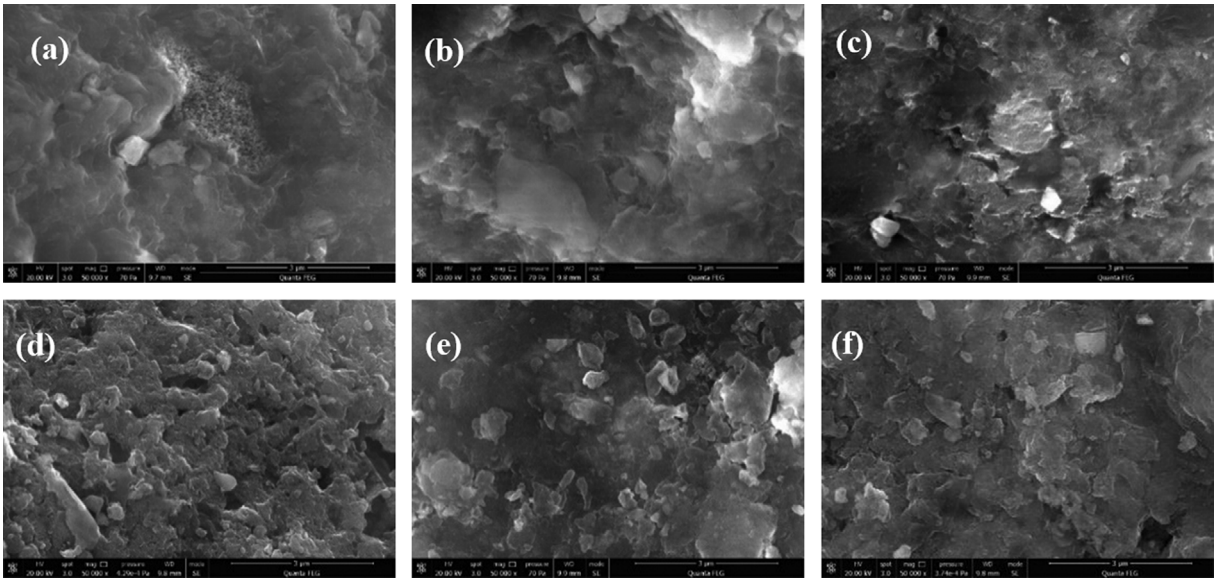

Fig. 2. SEM images (magnified 50 000 times) of raw sludge (a) and sludge cake treated by WSP (b), ZVI/PMS (c), ZVI/PMS-T (d), ZVI/PMS-T/pH (e) and ZVI/PMS/WSP-T/pH (f).

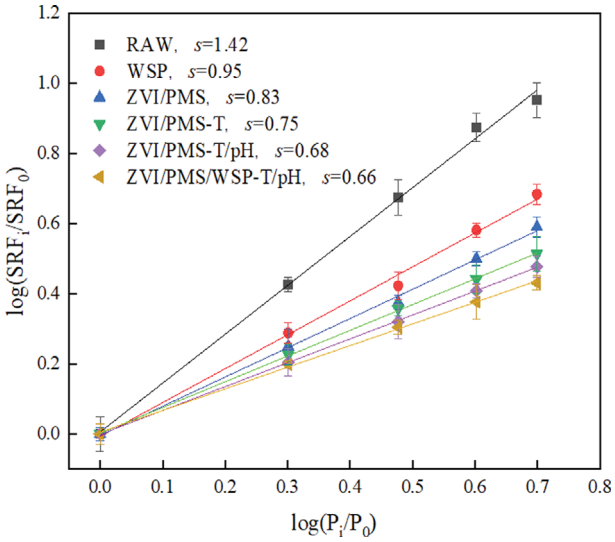

Fig. 3. Variations of sludge compressibility treated by different methods.

permeable channels and result in the inability of water discharge [43]. Fig. 3 shows that the *s* value of raw sludge was 1.42, and it decreased to 0.95 after using WSP. This indicated that WSP with rigid structure and porosity [44] could act as a skeleton builder to increase sludge incompressibility and form channels for water. When treated by ZVI/PMS and ZVI/PMS-T, the values of s decreased to 0.83 and 0.75, respectively, due to the bound water released under the oxidation of active species. The *s* value further decreased to 0.68 when conditioned by ZVI/PMS-T/pH. It was due to the broken sludge floc being re-agglomerated under the function of Fe^{3+} and Fe^{2+}.

As shown in Fig. 4(b), the total Fe content increased sharply in acidic conditions. When conditioned by ZVI/PMS/WSP-T/pH, under the combined functions of oxidation, re-aggregation and WSP as skeleton builder, the s value was reduced to 0.66, which was 53.52% lower than that of raw sludge. Cao et al. [45] and Li et al. [41] suggested that the lower s value usually indicated greater incompressibility of sludge, and it was conducive for water discharging. Thus, due to the rigid grid structure formed by WSP and flocs, the compressibility of the sludge conditioned by ZVI/PMS/WSP-T/pH reduced and the dewatering performance of the sludge reached the best.

4. Zeta Potential

Zeta potential is an essential element to characterize the dewaterability performance of sludge [3]. Due to negatively charged groups in EPS [8,46], the surface of sludge particles is usually negatively charged. The zeta potential of raw sludge was −22.13 mV (Fig. 4(a)), which was not conducive to aggregation and destabilization of the sludge [47]. The zeta potential decreased slightly when adding WSP due to the negatively charged powder [48]. However, the zeta potential continuously increased to −14.11 mV and −4.88 mV when conditioned by ZVI/PMS and ZVI/PMS-T. Under the strong oxidation of $SO_4^{-\bullet}$ and ·OH, the negatively charged EPS wrapped around the sludge cells was stripped off [49]. Moreover, the radicals and Fe^{3+} in ZVI/PMS-T system were more than that in ZVI/PMS system due to the combined activation of Fe^{2+} and thermal for PDS, and the thermal hydrolysis also conducive to EPS dissolution. Furthermore, when treated by ZVI/PMS-T/pH, the zeta potential value changed from negative to positive at 1.64 mV. It was because abundant positively Fe^{3+} and Fe^{2+} dissolved out under acid conditions, at 105.63 mg/L and 5.33 mg/L, which was more than in ZVI/PMS and ZVI/PMS-T systems (Fig. 4(b)). The positively charged Fe^{3+} and Fe^{2+} can effectively neutralize the negative surface charge of sludge floc to increase the zeta potential, even causing the increase of the zeta potential. On the other hand, the H^+ existing in acidic condition also could neutralize negative charge on sludge floc. Under this condition, the sludge was easy to aggregate and destabilize, and the sludge dewaterability was enhanced. For ZVI/PMS/WSP-T/pH system, due to the negatively charged on WSP surface, the zeta potential slightly decreased to −0.91 mV (Fig. 4(a)), and the positively charged Fe^{3+} and Fe^{2+} contents decreased to 101.75 mg/L and 5.06 mg/L (Fig. 4(b)). However, its absolutely value was still near zero, indicating the sludge dewater-

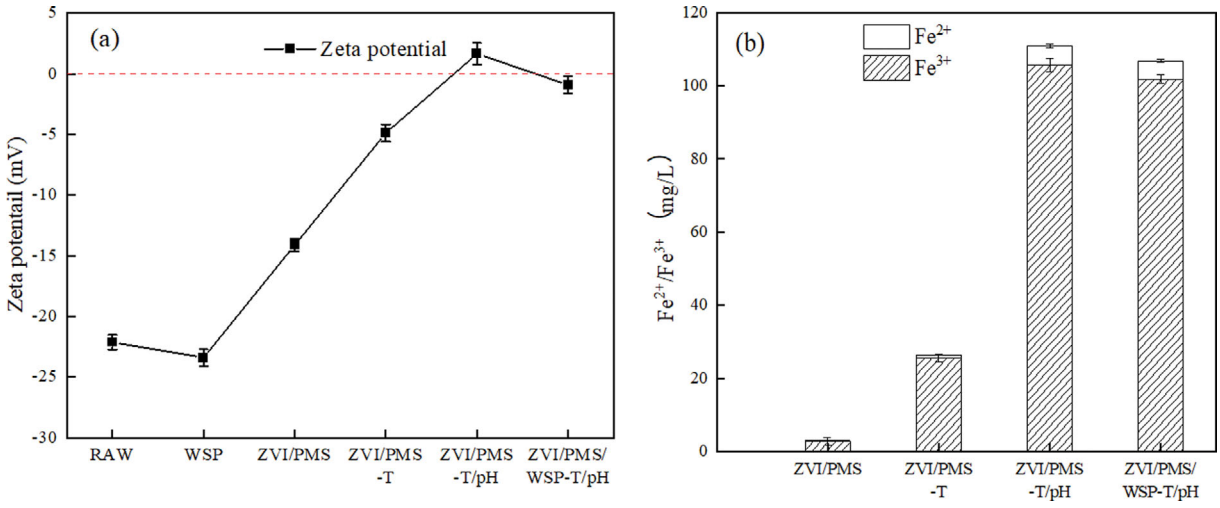

Fig. 4. The changes of zeta potential (a) and Fe^{2+}/Fe^{3+} contents (b) of sludge.

ing performance was successfully enhanced.

5. EPS Analysis

Sludge flocs and cells were bonded by EPS, which were mainly composed of polysaccharides (PS) and proteins (PN) [50], and had a multilayer structure with rheological properties [21]. The highly charged EPS decreased sludge dewatering efficiency due to its hydrophilic and viscous colloidal structure that holds water [46,51]. EPS included tightly bounded EPS (TB-EPS), loosely bonded EPS (LB-EPS) and soluble EPS (S-EPS) layers from inside to outside [37, 52]. Wang et al. [53] pointed out that TB-EPS is an important factor affecting the viscosity and stability of sludge flocs. Li et al. [41] reported that LB-EPS could have a crucial impact on improving of sludge flocculation performance. Thus, the destruction and degradation of EPS are significant in promoting the release of bound water from sludge floc and improving sludge dewaterability [21].

It can be seen from Fig. 5 that the contents of PN and PS in TB-EPS of raw sludge were 14.04 mg/g TS and 11.34 mg/g TS, respectively, which account for 81.82% PN and 77.14% PS. Except for the WSP system, the PN and PS in TB-EPS had decreased when pretreated using different chemical conditions. For ZVI/PMS and ZVI/PMS-T systems, PN and PS in TB-EPS degreased, and they were increased in LB-EPS and S-EPS. It indicated that the $SO_4^{-\bullet}$ and ·OH formed in ZVI/PMS and ZVI/PMS-T systems could effectively destroy TB-EPS and then transfer it into LB-EPS and S-EPS, thus breaking the sludge floc, bound water wrapped in EPS. For ZVI/PMS-T/pH and ZVI/PMS/WSP-T/pH systems, the PN and PS in TB-EPS, LB-EPS, and S-EPS decreased. Significantly, for TB-EPS, the PN and PS decreased to 5.67-5.73 mg/g TS and 3.11-3.52 mg/g TS and reduced by 66.61%-66.96% and 76.12%-78.90%, respectively, when compared with raw sludge. Moreover, the total EPS was reduced by 54.80% (ZVI/PMS-T/pH) and 51.10% (ZVI/PMS/WSP-T/pH). The decreased EPS appeared under the strong oxidation of $SO_4^{-\bullet}$ and ·OH, or the peeling off EPS fragments was flocculated by iron and then settled down.

It was reported that EPS, especially PN in EPS, could show better water retention capacity [27], so its degradation greatly improved sludge dewaterability. However, compared with ZVI/PMS-T/pH system, the EPS in ZVI/PMS/WSP-T/pH increased slightly, caused by the negative charged WSP. However, the slight change had little effect on sludge dewaterability.

6. Sludge Fractal Dimension

Fractal dimension is an essential parameter of sludge, describing its shape, spatial structure, self-similarity and size distribution [31,54,55]. It can be used to study the sludge dewatering performance, including dewaterability [56], CST [57] and bound water content [58]. Sludge floc with loose structure has a low fractal dimension. However, sludge floc with a large and dense structure usually has a high fractal dimension [54], better dewaterability and settleability.

The images of sludge floc after treatment and fractal dimensions after different treatment methods are shown in Figs. 6 and 7.

It can be seen that the raw sludge has a loose structure with a

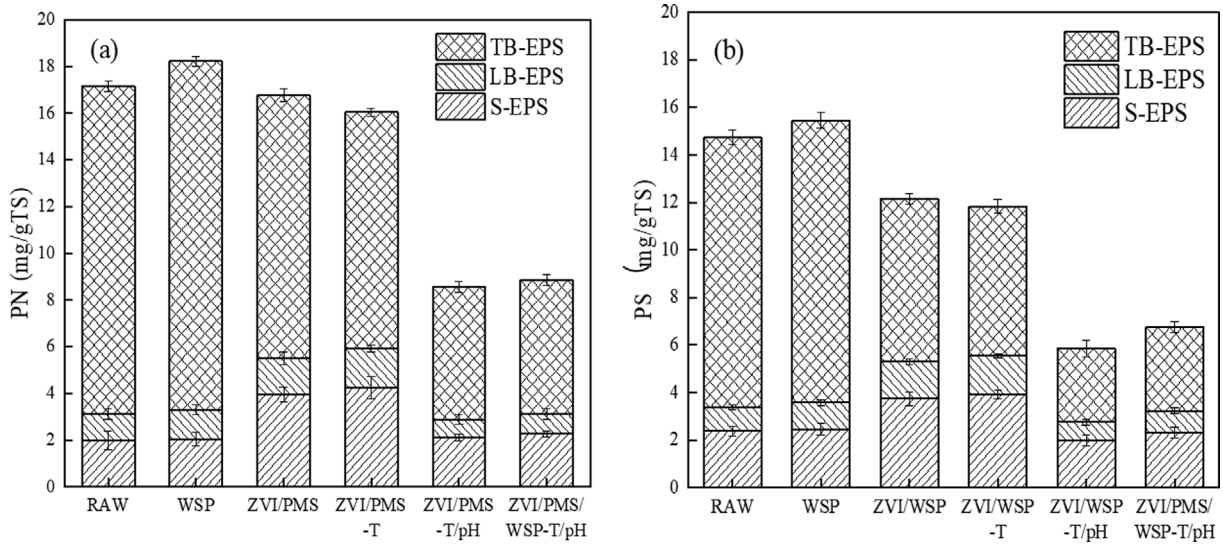

Fig. 5. The changes of the PN (a) and PS (b) in the EPS under different treatment conditions.

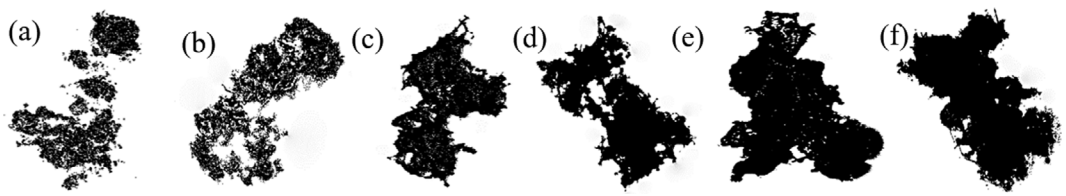

Fig. 6. Pixel images of sludge floc under different treatment conditions. (a)-RAW, (b)-WSP, (c)-ZVI/PMS, (d)-ZVI/PMS-T, (e)-ZVI/PMS-T/pH, (f)-ZVI/PMS/WSP-T/pH.

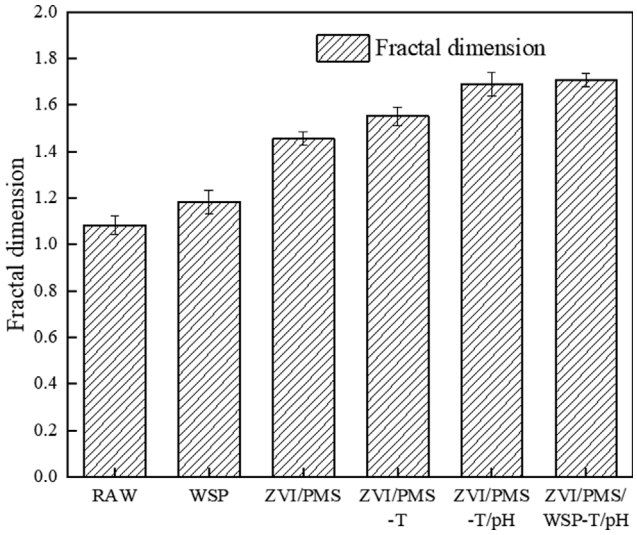

Fig. 7. Fractal dimension of sludge floc using different treatment conditions.

fractal dimension of 1.08. When treated with WSP, ZVI/PMS and ZVI/PMS-T, the sludge floc became more dense and compact, the internal porosity decreased until disappeared, and the fractal dimensions increased to 1.19, 1.46 and 1.55, respectively. For WSP, it cannot change the structure of sludge floc, but it can increase the density of sludge to increase the fractal dimensions. While for ZVI/PMS and ZVI/PMS-T, the sludge floc was broken under the strong oxidation of free radicals, the bound water released, electronegativity reduced, and sludge floc became dense. Large and dense sludge flocs were observed for ZVI/PMS-T/pH and ZVI/PMS/WSP-T/pH conditions; the corresponding fractal dimensions were 1.69 and 1.71, respectively, due to the re-flocculation of sludge fragments by Fe^{3+} and Fe^{2+}. The higher fractal dimension value of ZVI/PMS/WSP-T/pH was because WSP can fill in sludge floc to increase sludge density and aggregate with sludge floc through adsorption.

7. Sludge Dewatering Mechanism Analysis

According to the previously presented and discussed results, the mechanism of sludge dewatering treated by ZVI/PMS/WSP-T/pH can be described as follows: thermal and acid conditions promoted the corrosion of Fe^{2+} from ZVI, and then ZVI, Fe^{2+} and heat all can activate PMS to produce strong radicals of $SO_4^{-\bullet}$ and ·OH. During this process, the flocculants of Fe^{3+} were formed as a byproduct. Under the strong oxidation of these active species and acid and thermal hydrolysis, EPS, especially TB-EPS, was significantly decreased, sludge floc was destroyed, and bound water was released. The stripping of negatively EPS and neutralization of Fe^{2+}, Fe^{3+} and H^+ caused the absolute value of zeta potential to increase. WSP being negatively charged showed a lower zeta potential value, but it improved sludge compressibility and fractal dimension as a skeleton builder. Under the combined function of oxidation, acid/thermal hydrolysis, re-flocculation and skeleton builder, the sludge dewatering performance was greatly improved.

8. Economic Analysis

Economic analysis of ZVI/PMS/WSP-T/pH process was conducted, and the result was compared with those of ZVI/PMS and ascorbic acid (H_2A)-ZVI/PS processes. Although, the financial cost of ZVI/PMS/WSP-T/pH increased, the sludge dewatering efficiency was significantly improved. The W_c treated by ZVI/PMS/WSP-T/pH process was 62.1%, while for ZVI/PMS and H_2A-ZVI/PS processes, it was 80.5% and 75.6%, respectively (Table 2). Taking 100 m^3 of waste activated sludge with water content of 98% as the treatment object, the economic analysis result showed that the cost of ZVI/PMS/WSP-T/pH treatment was more expensive than that of ZVI/PMS and H_2A-ZVI/PS treatments, while for H_2A-ZVI/PS process it was calculated with the initial sludge water content of 94% [17]. In addition, the addition of WSP significantly increased the organic matter content in sludge cake and the calorific value of sludge, reduced the cost of subsequent sludge treatment by thermal drying or incineration, and it was also conducive to the utilization of sludge as a resource. Moreover, the low temperature (55 °C) and acidic conditions (pH 3) can effectively kill pathogenic bacteria, parasites and other harmful microorganisms, and realize harmless of sludge. Note that the aim of this paper was to improve the activation performance of ZVI for PMS in sludge conditioning and reveal its mechanism. In the future, further research is needed on its practical and financial feasibility in actual conditions.

CONCLUSIONS

ZVI/PMS/WSP-T/pH was used to condition sludge, and the

Table 2. Comparison of economic analysis between ZVI/PMS/WSP-T/pH, ZVI/PMS and H_2A-ZVI/PS treatments

Treatment methods	W_c	Reagent price	Reagent cost (¥)	Total cost (¥)	
ZVI/PMS/WSP-T/pH	62.1%	22 ¥/kg ZVI	5,082	10,684	This paper
		18 ¥/kg PMS	1,386		
		70 ¥/L HCl	560		
		0.5 ¥/kW·h	3,656		
ZVI/PMS	80.5%	22 ¥/kg ZVI	5,082	6,468	This paper
		18 ¥/kg PMS	1,386		
H_2A-ZVI/PS	75.6%		9,517	9,517	Ref. [17]

[a]This economic analysis was based on 100 m^3 waste activated sludge with 98% water content.

[b]W_c (water content of sludge cake by vacuum filtration with 0.1 MPa for 5 min) was measured in section 2.2 of this paper.

[c]The dosage of reagents was the same as that of this paper and the reagent price referred to the regent platform of HEBUT.

results were compared with WSP, ZVI/PMS, ZVI/PMS-T and ZVI/PMS-T/pH. After being treated by ZVI/PMS/WSP-T/pH, sludge dewatering performance improved significantly, CST and W_c were reduced to 6.8 s and 62.1%, and Y_N increased to 58.74 kg/(m^2·h). Mechanism analysis revealed that high temperature and low pH value could promote the corrosion of Fe^{2+} from ZVI, and then ZVI, Fe^{2+}, and thermal all can activate PMS to produce strong radicals of $SO_4^{\cdot-}$ and ·OH. These active species combined with acid and thermal could reduce EPS, especially TB-EPS, destroy sludge floc and release bound water. Meanwhile, the stripping off of EPS and the neutralization of Fe^{2+}, Fe^{3+} and H^+ caused the absolute value of zeta potential to increase, and sludge floc was destabilized with easy aggregation to dewater. The WSP with rigid structure and porosity could be used as a skeleton builder to increase sludge incompressibility and form channels for water. The s value was 53.52% lower than that of raw sludge. Under the aggregation of Fe^{3+} and the adsorption of WSP, the sludge floc became large and dense, and the fractal dimension increased to 1.71. Under the combined functions of oxidation, re-aggregation and skeleton builder, the sludge dewatering performance greatly improved. Nevertheless, there are still many details worthy of in-depth study to reduce the cost before the system is applied to actual sludge treatment.

ACKNOWLEDGEMENTS

The authors thank the financial support from the National Natural Science Foundation of China (22278100); Training Plan for Young Innovative Talents of Ordinary Undergraduate Colleges and Universities in Heilongjiang Province (No. UNPYSCT-2015046).

REFERENCES

1. X. H. Dai, *Science*, **72**(06), 30 (2020).
2. B. D. Cao, T. Zhang, W. J. Zhang and D. S. Wang, *Water Res.*, **189**, 116650 (2021).
3. Y. P. Zhang, T. T. Li, J. Y. Tian, H. C. Zhang, F. Li and J. H. Pei, *J. Environ. Sci.*, **113**, 152 (2022).
4. X. Y. Fan, Y. L. Wang, D. X. Zhang, Y. J. Guo, S. H. Gao, E. R. Li and H. L. Zheng, *J. Environ. Sci.*, **91**, 73 (2020).
5. T. Tunçal and A. S. Mujumdar, *Dry. Technol.*, **41**(3), 339 (2022).
6. T. Tunçal, *Dry. Technol.*, **40**(10), 2128 (2021).
7. M. Basuvaraj, J. Fein and S. N. Liss, *Water Res.*, **82**, 104 (2015).
8. B. B. Lan, R. F. Jin, G. F. Liu, B. Dong, J. T. Zhou and D. F. Xing, *Water Environ. Res.*, **93**(9), 1680 (2021).
9. U. Menon, N. Suresh, G. George, A. M. Ealias and M. P. Saravanakumar, *Chem. Eng. J.*, **382**, 123035 (2020).
10. L. Y. Liu, H. Yan, C. Yang and G. R. Zhu, *RSC Adv.*, **8**(52), 29756 (2018).
11. G. B. Gholikandi, N. Zakizadeh and H. Masihi, *J. Environ. Manage.*, **206**, 523 (2018).
12. T. Tunçal, İ. Ç. Deniz and U. Orhan, *Appl. Catal. B-Environ.*, **179**, 171 (2015).
13. D. W. T. Li, J. R. Lv, Z. M. Qiang and M. K. Li, *J. Hazard. Mater.*, **391**, 121855 (2020).
14. C. G. Liu, B. Wu and X. E. Chen, *Chem. Eng. J.*, **335**, 865 (2018).
15. C. G. Liu, *Chem. Eng. J.*, **359**, 217 (2019).
16. X. Ling, M. J. Chen, A. H. Cai, H. L. Sun, S. L. Xu, L. Wang, X. Y. Li and J. Deng, *J. Environ. Manage.*, **318**, 115646 (2022).
17. L. H. Yuan, H. X. Liu, Y. J. Lu, Y. Lu and D. B. Wang, *Chemosphere*, **303**, 135104 (2022).
18. J. L. Liang, L. Zhang, W. W. Yan and Y. Zhou, *Water Res.*, **184**, 116149 (2020).
19. R. H. Ramachandra and C. P. Devatha, *Environ. Sci. Pollut. R.*, **27**(11), 11870 (2020).
20. H. Wei, B. Q. Gao, J. Ren, A. M. Li and H. Yang, *Water Res.*, **143**, 608 (2018).
21. Q. X. Dai, L. P. Ma, N. Q. Ren, P. Ning, Z. Y. Guo, L. G. Xie and H. J. Gao, *Water Res.*, **142**, 337 (2018).
22. W. Wu, Z. Zhou, J. Z. Yang, G. Chen, J. Yao, C. Q. Tu, X. D. Zhao, Z. Qiu and Z. C. Wu, *Water Res.*, **160**, 167 (2019).
23. Y. Wu, P. Y. Zhang, G. M. Zeng, J. Ye, H. B. Zhang, W. Fang and J. B. Liu, *ACS Sustainable Chem. Eng.*, **4**(10), 5711 (2016).
24. X. X. Geng, S. Y. Lv, J. Yang, S. H. Cui and Z. H. Zhao, *J. Environ. Manage.*, **280**, 111749 (2021).
25. B. W. Wang and Y. Wang, *Sci. Total Environ.*, **831**, 154906 (2022).
26. APHA, *Standard methods for the examination of water and wastewater*, 21st ed. Washington: American Public Health Association (2015).
27. J. Liu, Q. Yang, D. B. Wang, X. M. Li, Y. Zhong, X. Li, Y. C. Deng, L. Q. Wang, K. X. Yi and G. M. Zeng, *Bioresour. Technol.*, **206**, 134 (2016).
28. K. Grintzalis, C. D. Georgiou and Y. J. Schneider, *Anal. Biochem.*, **480**, 28 (2015).
29. T. Zavrel, P. Ocenasova, M. A. Sinetova and J. cerveny, *Bio-protocol*, **8**(15), e2966 (2018).
30. S. Felz, P. Vermeulen, M. C. M. Van Loosdrecht and Y. M. Lin, *Water Res.*, **157**, 201 (2019).
31. Z. H. Li, Y. Guo, Z. Y. Hang, T. Y. Zhang and H. Q. Yu, *Water Res.*, **178**, 115834 (2020).
32. H. Wei, J. Ren, A. M. Li and H. Yang, *Chem. Eng. J.*, **349**, 737 (2018).
33. Y. F. Li, L. Y. Pan, Y. Q. Zhu, Y. Y. Yu, D. B. Wang, G. J. Yang, X. Z. Yuan, X. R. Liu, H. L. Li and J. Zhang, *Water Res.*, **163**, 114912 (2019).
34. X. Zhou, Q. L. Wang, G. G. Jiang, P. Liu and Z. G. Yuan, *Bioresour. Technol.*, **185**, 416 (2015).
35. C. G. Liu, B. Wu and X. E. Chen, *Chem. Eng. J.*, **392**, 124850 (2020).
36. M. Q. Wang, Y. Wu, B. R. Yang, P. Y. Deng, Y. H. Zhong, C. Fu, Z. H. Lu, P. Y. Zhang, J. Q. Wang and Y. Y. Qu, *Sci. Rep-UK*, **10**(1), 17230 (2020).
37. X. D. Zhang, P. Ye and Y. J. Wu, *J. Environ. Manage.*, **321**, 115938 (2022).
38. W. Burger, K. Krysiak-Baltyn, P. J. Scales, G. J. O. Martin, A. D. Stickland and S. L. Gras, *Water Res.*, **123**, 578 (2017).
39. Y. F. Li, X. Z. Yuan, D. B. Wang, H. Wang, Z. B. Wu, L. B. Jiang, D. Mo, G. J. Yang, R. P. Guan and G. M. Zeng, *Bioresour. Technol.*, **262**, 294 (2018).
40. M. Banerjee, N. Bar and S. K. Das, *Int. J. Environ. Res.*, **15**(5), 875 (2021).
41. L. X. Li, C. Peng, L. H. Deng, F. G. Zhang, D. Wu, F. Ma and Y. Liu, *J. Environ. Manage.*, **301**, 113926 (2022).
42. P. Hu, S. H. Zhuang, S. H. Shen, Y. H. Yang and H. Yang, *Water Res.*, **189**, 116578 (2021).

43. X. C. Zhang, H. S. Kang, Q. R. Zhang, X. M. Hao, X. Han, W. Zhang and T. F. Jiao, *J. Environ. Manage.*, **230**, 14 (2019).
44. S. D. Guo, F. S. Qu, A. Ding, J. G. He, H. R. Yu, L. M. Bai, G. B. Li and H. Liang, *RSC Adv.*, **5**(54), 43065 (2015).
45. B. D. Cao, W. J. Zhang, Q. D. Wang, Y. R. Huang, C. R. Meng and D. S. Wang, *Water Res.*, **105**, 615 (2016).
46. L. L. Wei, X. H. Xia, F. Y. Zhu, Q. Y. Li, M. Xue, J. J. Li, B. Sun, J. Q. Jiang and Q. L. Zhao, *Water Res.*, **181**, 115903 (2020).
47. J. Y. Guo, Q. F. Gao, Y. H. Chen, Q. L. He, H. B. Zhou, J. B. Liu, C. W. Zou and W. J. Chen, *J. Environ. Manage.*, **288**, 112476 (2021).
48. M. K. Uddin and A. Nasar, *Sci. Rep-UK*, **10**(1), 7983 (2020).
49. C. G. Liu, X. E. Chen and H. T. Cai, *Chem. Eng. J.*, **400**, 125954 (2020).
50. F. Lin, X. L. Zhu, J. G. Li, P. R. Yu, Y. Luo and M. R. Liu, *Chemosphere*, **235**, 679 (2019).
51. V. H. P. To, T. V. Nguyen, H. Bustamante and S. Vigneswaran, *Sep. Purif. Technol.*, **239**, 116557 (2020).
52. X. R. Liu, X. D. Huang, Y. X. Wu, Q. X. Xu, M. T. Du, D. B. Wang, Q. Yang, Y. W. Liu, B.-J. Ni, G. J. Yang, F. Yang and Q. L. Wang, *Chem. Eng. J.*, **387**, 124147 (2020).
53. S. Wang, X. X. Ma, Y. Y. Wang, G. C. Du, J.-H. Tay and J. Li, *Bioresour. Technol.*, **273**, 350 (2019).
54. H. T. Fan, X. H. Liu, H. Wang, Y. P. Han, L. Qi and H. C. Wang, *Chemosphere*, **169**, 586 (2017).
55. N. Wang, W. J. Zhang, B. D. Cao, P. Yang, F. G. Cui and D. S. Wang, *Chem. Eng. J.*, **350**, 660 (2018).
56. J. S. Zhang, N. Li, X. H. Dai, W. Q. Tao, I. R. Jenkinson and Z. Li, *Water Res.*, **131**, 177 (2018).
57. Y. D. Zheng, M. Y. Xing, L. Z. Y. Cai, T. Xiao, Y. F. Lu and J. Z. Jiang, *Sci. Total Environ.*, **581**, 573 (2017).
58. B. R. Wu, H. Wang, X. H. Dai and X. L. Chai, *Water Res.*, **202**, 117461 (2021).